JOURNAL OF NANO- AND ELECTRONIC PHYSICS
Vol. **7** No 1, 01040(5pp) (2015)

ЖУРНАЛ НАНО- ТА ЕЛЕКТРОННОЇ ФІЗИКИ
Том **7** № 1, 01040(5cc) (2015)

The Influence of the Ion Implantation of Au^- to the Microstructure of the Amorphous-nanocrystaline AlN-TiB_2-$TiSi_2$

K.V. Smyrnova[1,*], A.A. Demianenko[1], K.A. Dyadyura[1], A.S. Radko[1], A.V. Pshyk[1,2], O.V. Kuzovlev[3], H. Amekura[4], K. Oyoshi[4], Y. Takeda[4]

[1] *Sumy State University, 2, Rimsky-Korsakov Str., 40007 Sumy, Ukraine*
[2] *Adam Mickiewicz University in Poznan, NanoBioMedical Centre, PL61614 Poznan, Poland*
[3] *V. N. Karazin Kharkiv National University, 4, Svobody Sq., 61022, Kharkiv, Ukraine*
[4] *National Institute for Material Science (NIMS), 305-0047, Tsukuba, Ibaraki, Japan*

(Received 04 February 2015; revised manuscript received 16 March 2015; published online 25 March 2015)

Direct measurements were performed using TEM, HRTEM, XRD and SEM with microanalysis. The results showed that the thermal annealing at 1300 °C in air leads to the formation of nanoscale phases 10÷15 nm from AlN, AlB_2, Al_2O_3 and TiO_2. Moreover, the ion implantation of the negative ions Au^- causes fragmentation (decrease) of the size of nanograins to 2-5 nm with the formation of Au^- clusters. In addition, the ion implantation leads to the formation of an amorphous oxide film in the depth (at the undersurface layer) of the coating.

Keywords: Ion implantation, Nanocrystallites, Amorphous structures, Vacancy Loops, Interstitial types.

PACS numbers: 52.77.Dq, 61.72.uj, 81.07.Bc

1. INTRODUCTION

The implantation of intense beams of the negative ions has recently received a significant development due to the creation of this type of accelerators, and their successful application [1, 2]. For example, doping of the dielectrics (SiO_2) is used for obtaining the radiation of the ultraviolet range (using luminescence). The emission centers in such doped dielectrics are the nanoparticles, which formed from Au and Cu ions as the result of the implantation [2].

At the same time the undoubted advantage of the negative ions is that the process of their implantation into the dielectric doesn't lead to its charging. On the other hand, nanocomposites (or nanomaterials) together with a high hardness (and also the plasticity) must possess a high resistance to the thermal oxidation [3, 4]. In addition, the formation of an amorphous-like structure in the multicomponent (gradient) coatings is an important factor [5]

It determines their high functional properties and a high diffusion resistance to external influences. It is possible due to the lack of the ways of easy diffusion in the amorphous-like matrix. Certainly, the amorphous-like structures are thermodynamically metastable, and therefore an important factor of their restructuring is annealing at high temperatures. At the same time, the implantation high doses of heavy ions up to 10^{17} cm^{-2} in the amorphous-nanocrystalline structure is insufficiently explored. Due to it we have to serve the problem of studying of these processes which occurs in such structures after implantation of the energetic ions.

2. EXPERIMENT

The coatings were deposited on polished Mo and Si samples using pulsed magnetron sputtering on the target with complex composition of AlN-TiB_2-$TiSi_2$ (30 %). The elemental composition and the surface morphology of the coatings were determined using JEOL-7000F with microanalysis. The structure and substructure of the coated samples were investigated by the method of small-angle scattering of Cr-Kα radiation using diffractometer RINT-2500V. The surveying was performed with the scattering angles 2°, 3°, 10° and 30°. The atomic structure of the samples was explored using the electron microscope JEOL JEM-2100F in the bright and dark field.

Negative ions of Au^- were generated by a Cs^- assisted heavy ion source of plasma-sputter type with a cusp magnetic field, as illustrated in fig.1. The negative heavy ion source has been established by Nissan High Voltage Co. Ltd [2].

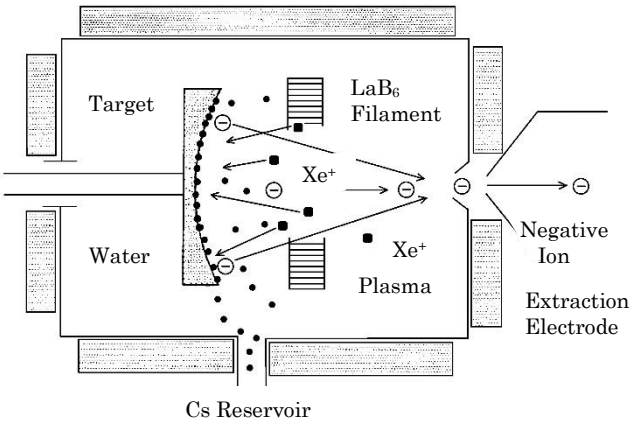

Fig. 1 – Negative heavy ion source of plasma-sputter type with a cusp magnetic fields

The intense ion beam of the negative ions was formed by two electrodes and accelerated up to – 60 keV (beam current ≤ 4 mA). The system employed a VPQM (variable permanent quadrupole-magnets) triplet and

* smyrnova_katerina@ukr.net

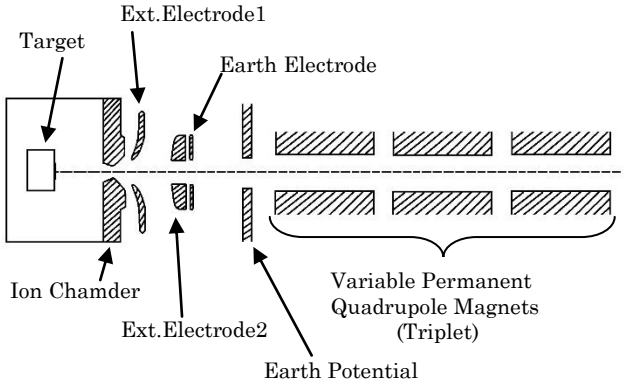

Fig. 2 – Schematic chart of the baem transport (the upstream part) in the ntgative-ion implanter

the beam optics was optimized including those lenses, as shown in Fig. 2 [2].

3. RESULTS AND DISCUSSION

The results of the elemental composition of the AlN-TiB_2-$TiSi_2$ coatings in the as-deposital state and after annealing at 900 °C and 1300 °C are given in the Table 1. It can be seen that with increasing of the annealing temperature the concentration of B decreased from 34 to 23.37 at. %, N from 9.26 to 6.97 at. %, Al from 17.25 to 14.45 at. %, Si from 2.89 to 0.32 at. %, Ti from 6.92 to 0.49 at. %. At the same time, the growth of C concentration from 17.27 to 30.36 at. %, Oxygen from 11.52 to 26.84 at. % is observed.

Table 1 – The results of the elemental composition of the coatings AlN-TiB_2-$TiSi_2$ in the initial state and after annealing at 900 °C and 1300 °C

Annealing temperature, °C	Elements included to the coating composition, at.%						
	B	C	O	N	Al	Si	Ti
–	34.49	17.27	11.92	9.26	17.25	2.89	6.92
900	38.07	12.70	13.14	8.32	18.30	2.70	6.72
1300	23.57	30.36	26.84	6.97	11.45	0.32	0.49

The results obtained by XRD (Fig. 3a) and their analysis demonstrated that during the deposition process the coating with X-ray amorphous structure is formed [6]. This conclusion is also confirmed by TEM and HRTEM analysis. Radiographs at angles 30-50 degrees and 65-75 degrees show a halo with a maximum (at the absence of clearly defined diffraction peaks). Evaluation of the area of short-range order of the ordering in the coatings is performed using the equation:

$$R_m \approx \frac{10}{\Delta s} \qquad (3.1)$$

where Δs is the width of the first wide-angle «galo-like» curve in the coordinates of "intensity – scattering vector **s**» (modulus of the scattering vector $s = |\vec{\mathbf{s}}| = 4\pi \sin\theta / \lambda$). It shows that the regions of ordering are around $R_m = 10$ Å = 1 nm.

It should be noted that equation (3.1) follows from the fact that the correlation (the value of the area of the ordering) is inversely proportional to Δs:

$$R_m = \frac{2\pi^3 z^2}{6{,}25\Delta s} \qquad (3.2)$$

where z is the index of the maximum. For the first peak ($z = 1$) $R_m \approx 10 / \Delta s$.

Annealing at higher temperature (1300 °C) leads to a fundamental change in the picture of the diffraction pattern. Nanoscale phases of the aluminum oxide Al_2O_3, considerably less AlB_2 are formed in the coating [7]. In addition, β-TiO_2 in small quantities, AlN, and «perhaps» SiO_2 are found [8]. The greatest heat of the formation that is typical for these phases in this case causes the formation of AlB_2 and Al_2O_3 crystallites [9]. It should be noted that, in the case of annealing at 1300 °C and at the ion irradiation by Au^- (due to the etching of the surface and less linking energy) the surface of the coating is impoverished by the boride phase. It is proved by the relative decrease of the peaks obtained from aluminum diboride. There is also a decrease of the roughness. It is noticeably in a relatively low background scatter of the diffraction spectrum, which was obtained in the sliding geometry. However, near the surface of the a thin amorphous oxide film was formed. It is clearly seen on the cross-section of the coated sample and it is shown in figures below.

The results of the integral analysis on a section of coating of AlN-TiB_2-$TiSi_2$ after annealing at 1300 °C and implantation by Au^- with dose 10^{17} cm^{-2} are shown in the Table 2. As seen from these results, the concentration of the elements, which include in the composition of the coating, differs from the results of an analysis obtained from the surface of the coating. The concentration of the gold in this integral layer is 0.4 at. %. This gold layer is located in a depth from the surface approximately equal to R_p. It can be seen on the Fig. 3.

Fig. 3b shows the results of elemental analysis of the composition in the form of maps of the distribution of elements in the section of the sample in the elemental contrast and bright field. These maps demonstrate that C, Al, Ti, Si are uniformly distributed, besides the surface. In addition, the concentration of the oxygen is larger near the surface. The trace of Au, lying in a depth of the coating with the concentration of about 0.4 at. % is clearly seen. Fig. 4 shows a sectional view of the coating (in the bright field) obtained at 50000 times magnification in (resolution of about 20 nm). This figure clearly shows that the coating consists of three layers [10]. The first is under layer C, with sizes of the crystallites up to 10 nm, the following second layer is an amorphous oxide layer. Apparently, the second layer is disordered due to the ion
implantation of Au^- with doses 10^{17} cm^{-2}. After this layer follows another with nanoscale grains surrounded by an amorphous interlayer. This layer was formed due to the ballistic mixing of the oxide film from the surface.

Fig. 4 shows the results of TEM and HRTEM analysis of different regions of the coatings at different depths. A very fine-grained structure with typical sizes of nanograins (2-3 nm) formed in the first layer, obtained of the result of the implantation of the negative Au^- ions with 10^{17} cm^{-2} doses [11]. The process of implantation occurs with the formation of a high density of the

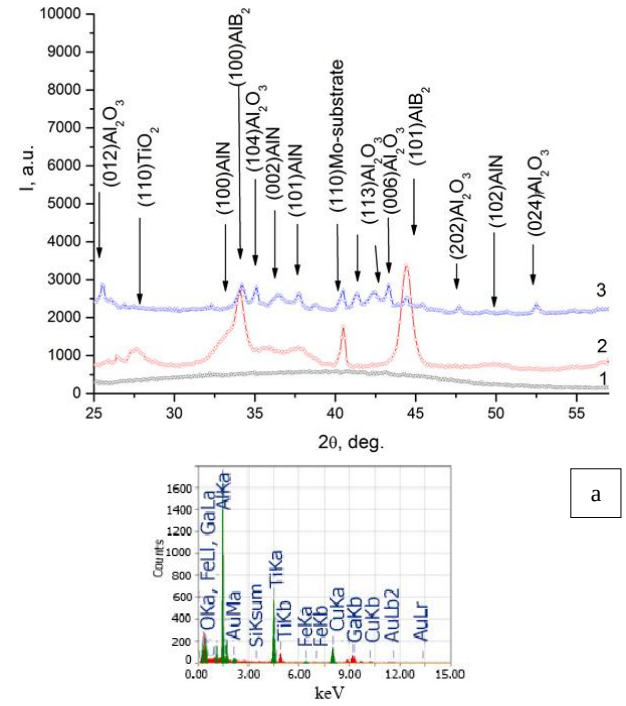

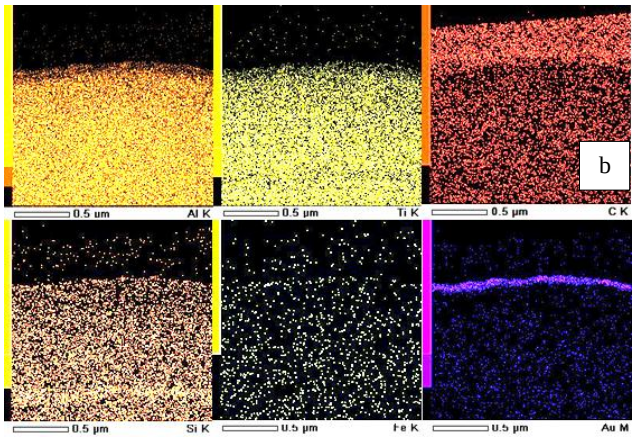

Fig. 3 – (a) the areas of radiographs of the coatings based on the AlN-TiB_2-$TiSi_2$: 1 – original state, 2 – annealing at 900 °C, 3 – at 1300 °C; (b) the results of the elemental analysis of elements Al, Ti, C, Si, Fe Au in the form of maps of the elemental distribution over the cross section of the sample in elemental contrast

individual cascades of the displaced atoms. So this is the reason for the formation of defects with a high efficiency: the loops of the vacancy and the interstitial types [12, 13]. Implanted Au ions in the coating form «ball-shape» nanocrystals – «spheroids» with sizes of about a few nanometers. Firstly, it was shown in the works devoted to implantation of the ions of Cu^- and Au^- in SiO_2 [2, 14].

The micro-diffraction of the area indicated on the Fig. 4a is shown in the right corner. As it can be seen it is the diffraction from particles (clusters of Au) implanted into the nanoscale matrix of the coating. The lattice parameters indicate the formation of the amorphous structure.

Table 2 – The results of the integrated analysis on a cut of the coating AlN-TiB_2-$TiSi_2$ after annealing at 1300 °C and implantation Au^- with doses 10^{17} cm^{-2}

Element	*E*, keV	Weight %	Mistake, %	At. %
O K	0.525	8.1	0.04	15.3
Al K	1.486	51.4	0.01	57.7
Si K	1.739	5.7	0.08	6.2
Ti K	4.508	31.7	0.02	20.0
Fe K	6.398	0.7	1	0.4
Au K	2.12	2.3	0.88	0.4
Totally		100.0		100.0

The following Fig. 4b shows an intermediate area which is located between the implanted region and the amorphous oxide layer. This area is also characterized by the small size of nanograins (2-3 nm), which are surrounded by the amorphous oxide interlayer. Under this structure an amorphous interlayer is located. Fig. 4c shows the image of the amorphous area (oxides). The right corner of Fig. 4c shows the diffraction of this field, that testifies about the amorphization of the layer. Oxide layer is located below the surface layer, which was formed due to the implantation of the heavy negative Au^- ions. The ballistic mixing of the surface layer (oxide) forms this layer. The surface layer formed as the result of annealing in the air. It is well known that a sufficient dose for mooving a thin layer to the depth of the mileage of ions (inert gases) is only 10^{16} cm^{-2} (it is almost an order of magnitude less than the implantation dose of Au^-). In consequence of implantation of Au^- ions with doses 10^{17} cm^{-2}, the surface oxide film «moves». It occurs by collisions due to the tight cascades. This surface oxide film moves to the depth close to R_p of Au. There is a process of the mass transfer of ions (atoms) to the depth of the nanocomposite film.

The coating is nanocomposite (there are several phases and the amorphous interlayer). Therefore the efficiency of the recombination of point defects increases near cascades (or inside of them) and because of the proximity of interfaces of nanograins, double, triple junctions [15]. Moreover, grinding (crushing) of the nanograins occur due to the collision of the heavy Au^- ions with atoms of the AlN-TiB_2-$TiSi_2$ coating. They become significantly smaller from (10-15) nm to (2-5) nm than they were obtained by the thermal annealing.

4. CONCLUSIONS

The structure of the X-ray amorphous coating, deposited from AlN-TiB_2-$TiSi_2$, was recrystallized using the negative ion beam of Au^- and the high-temperature annealing at 1300 °C. The formation of nanoscale phases and a decrease of the surface roughness with the formation of the thin amorphous oxide film are observed during annealing. Implantation of the negative ions reduces sizes of the nanograins due to the collisions of the Au^-ions with atoms of the X-rays coating. Implantation and annealing leads to the formation of three layers: the implanted area (amorphous), the intermediate layer and the amorphous oxide layer.

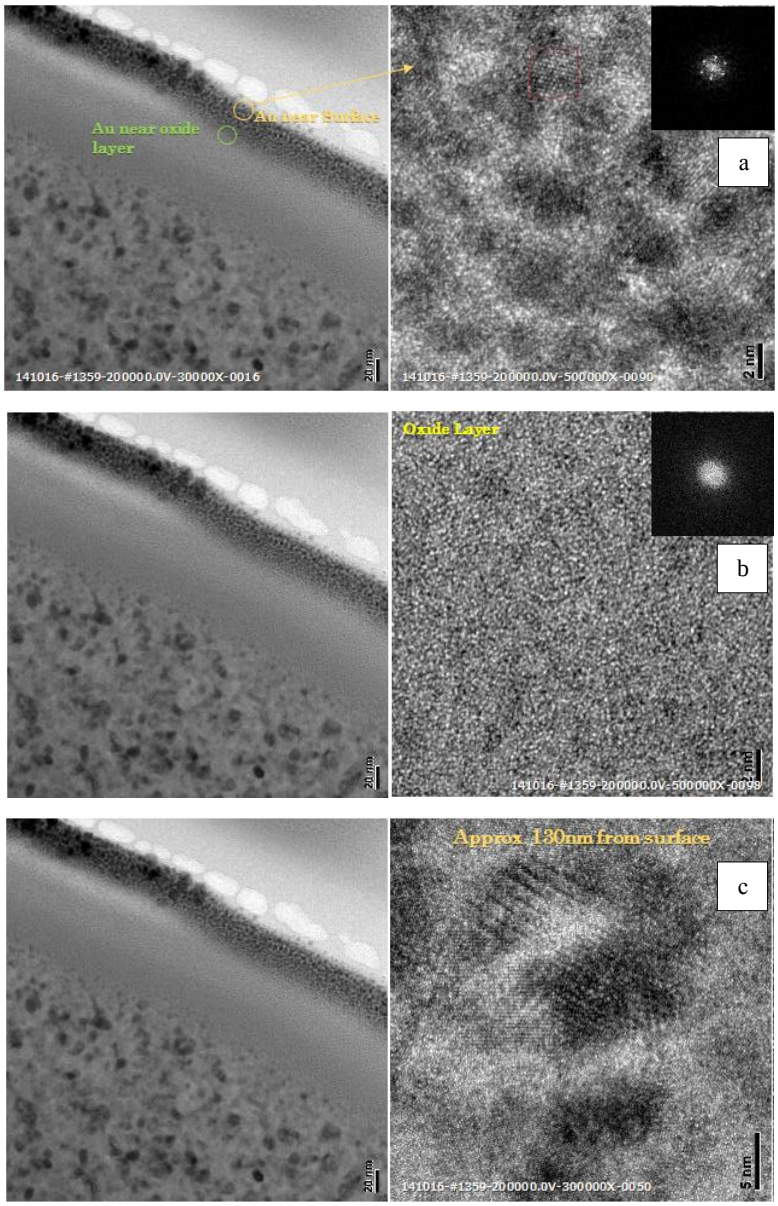

Fig. 4 – The results of TEM and HRTEM analysis: (a) the image of Au near the surface layer; (b) the image of the oxide layer; (c) images of the coating layer at the depth 130 nm from the surface

AKNOWLEDGENTS

The authors would like to thank Prof. Alexander Pogrebnjak, Prof. Oleg Sobol (Kharkiv National Technical University, Ukraine), Prof. Stefan Jurga (Adam Mickiewicz University in Poznan, Poland) for helping with the experiments and interpretation of results. The work was performed within the framework of budget state program "Development of the basis for formation of multicomponent nanostructured superhard coatings with high physical and mechanical properties" (No 0112U001382) and "Physical principles of plasma technologies for complex processing of multicomponent materials and coatings" (No 0113U000137c).

Влияние ионной имплантации Au^- на микроструктуру аморфно-нанокристаллического AlN-TiB_2-$TiSi_2$

Е.В. Смирнова[1], А.А. Демьяненко[1], К.А. Дядюра[1], А.С. Радько[1], А.В. Пшик[1,2], О.В. Кузовлев[3], Х. Амекура[4], К. Ойоши[4], Й. Такеда[4]

[1] *Сумский государственный университет, ул. Римского-Корсакова, 2, 40007 Сумы, Украина*
[2] *Университет имени Адама Мицкевича в Познани, НаноБиоМедицинсий Центр, PL61614 Познань, Польша*
[3] *Харьковский государственный университет им. В.Н. Каразина, пл. Свободы 4, 61022 Харьков, Украина*
[4] *Национальный институт материаловедения (NIMS), 1-2-1 Сенген, 305-0047 Цукуба, Ибараки, Япония*

Прямые измерения с помощью TEM, HRTEM, XRD и SEM с микроанализом показали, что термический отжиг 1300 °C на воздухе приводит к образованию наноразмерных фаз 10÷15 нм из AlN, AlB_2, Al_2O_3 и TiO_2, а ионная имплантация отрицательных ионов Au^- приводит к фрагментации (уменьшению) размеров нанозерен до 2-5 нм с образованием «сфероидов» из Au^- и формированию аморфной оксидной пленки в глубине (приповерхностном слое) покрытия.

Ключевые слова: Ионная имплантация, Нанокристаллиты, Аморфная структура, Петли вакансионного и межузельного типа.

Вплив іонної імплатнації Au^- на мікроструктуру аморфно-нанокристалічного AlN-TiB_2-$TiSi_2$

К.В. Смирнова[1], А.А. Дем'яненко[1], К.А. Дядюра[1], А.С. Радько[1], А.В. Пшик[1,2], О.В. Кузовлєв[3], Х. Амекура[4], К. Ойоши[4], Й. Такеда[4]

[1] *Сумський державний університет, вул. Римського-Корсакова, 2, 40007 Суми, Україна*
[2] *Університет ім. Адама Міцкевича в Познані, НаноБіоМедичний Центр, PL61614 Познань, Польща*
[3] *Харківський державний університет ім. В.Н. Каразіна, пл.Свободи 4, 61022 Харків, Україна*
[4] *Національний інститут матеріалознавства (NIMS), 1-2-1 Сенген, 305-0047 Цукуба, Ібаракі, Японія*

Прямі вимірювання за допомогою TEM, HRTEM, XRD и SEM з мікроаналізом показали, що термічний відпал при 1300 °C на повітрі призводить до утворення нанорозмірних фаз 10÷15 нм з AlN, AlB_2, Al_2O_3 і TiO_2, а іонна імплантація негативних іонів Au^- призводить до фрагментації (зменшення) розмірів нанозерен до 2-5 нм з утворенням «сфероїдів» з Au^- і формуванню аморфної оксидної плівки в глибині (приповерхневому шарі) покриття.

Ключові слова: Іонна імплантація, Нанокристаліти, Аморфна структура, Петлі вакансійного та міжвузельного типу.

REFERENCES

1. A.D. Pogrebnjak, Sh.M. Ruzimov, D.L. Alontseva, P. Zukowski, C. Karwat, C. Kozak, M.B. Kolasik, *Vacuum* **81**, 1243 (2007).
2. D. Debi, Y. Takeda, H. Amekura, *Appl. Surf. Sci.* **310**, 164 (2014).
3. A.D. Pogrebnjak, I.V. Yakushchenko, A.A. Bagdasaryan, *Mater. Chem. Phys.* **147**, 1079 (2014).
4. A.D. Pogrebnjak, A.A. Bagdasaryan, I.V. Yakushchenko, *Rus. Chem. Rev.* **83** No 11, 1027 (2014).
5. J. Musil, *Surf. Coat. Tech.* **207**, 50 (2012).
6. A.D. Pogrebnyak, A.V. Pshyk, V.M. Beresnev, B.R. Zhollybekov, *J. Frict. Wear+* **35** No 1, 55 (2014).
7. A.D. Pogrebnjak, M. Il'jashenko, O.P. Kul'ment'eva, V.S. Kshnjakin, A.P. Kobzev, Y.N. Tyurin, O.G. Kolisnichenko, *Vacuum* **62**, 21 (2001).
8. A.D. Pogrebnjak, Yu.A. Kravchenko, S.B. Kislitsyn, Sh.M. Ruzimov, F. Noli, P. Misaelides, A. Hatzidimitriou, *Surf. Coat. Tech.* **201**, 2621 (2006).
9. O.V. Sobol', A.D. Pogrebnyak, V.M. Beresnev, *Phys. Met. Metallogr+* **112** No 2, 188 (2011).
10. O.M. Ivasishin, A.D. Pogrebnjak, S.N. Bratushka, *Nanostructured Layers and Coating Formed by Ion-Plasma Fluxes in Titanium Alloys and Steels* (Kyiv: Akademperiodika: 2011).
11. A.D. Pogrebnjak, E.A. Bazyl, *Vacuum* **64**, 1 (2001).
12. F.F. Komarov, *Ion Implantation into Metals* (Moskow: Metallurgy: 1990).
13. A.D. Pogrebnjak, S.N. Bratushka, V.M. Beresnev, N. Levintant-Zayonts, *Rus. Chem. Rev.* **82** No 12, 1135 (2013).
14. N. Kishimoto, V.T. Gritsyna, Y. Takeda, C.G. Lee, *MRS Proceedings.* **504**, 345 (1997).
15. V. Ivashchenko, S. Veprek, A. Pogrebnjak, B. Postolnyi, *Sci. Technol. Adv. Mat.* **15** No 2, 025007 (2014).